Computational Materials Science 230 (2023) 112433

Contents lists available at ScienceDirect

Computational Materials Science

journal homepage: www.elsevier.com/locate/commatsci

Full length article

Atomistic study of hydrogen diffusion in presence of defects in bcc and fcc iron

D. Smirnova [*,1], S. Starikov

ICAMS, Ruhr-Universität Bochum, Universitätsstraße 150, 44801, Bochum, Germany

ARTICLE INFO

Keywords:
Hydrogen embrittlement
Iron
Hydrogen
Diffusion
Grain boundary

ABSTRACT

We present classical atomistic study of hydrogen diffusion in α-Fe and γ-Fe in presence of grain boundaries, surfaces or vacancies. Being pronounced traps for hydrogen, defects of different complexion play an important role in diffusion mechanisms related to hydrogen embrittlement. Clarification of hydrogen interaction with isolated defects is a necessary step towards establishing the hierarchy of related diffusion coefficients. We estimated possible impact of the above-mentioned defects on the H diffusion using recently developed interatomic potential capable of simulations of α and γ Fe phases. From the classical simulations we found that H interplay with defects may strongly depend on the host Fe structure: in fcc Fe, grain boundaries and surfaces provide accelerating path for diffusion, while in bcc we see no such effect. In case of a mono-vacancy, binding with hydrogen leads to reduction in a vacancy migration rate for both lattice types. However atomistic mechanisms of such slow-down are different. For bcc Fe we also estimated equilibrium hydrogen concentrations at grain boundaries and discuss a role of hydrogen located in GBs in overall hydrogen flux in polycrystal.

1. Introduction

Hydrogen embrittlement (HE) is a stand-alone topic in material science considering various aspects of materials degradation due to presence of hydrogen. For such widely used materials as steels, observed loss of material ductility and strength associated with hydrogen accumulation remains a noticeable technological limitation. Hence, research aimed at overcoming HE of steels initiates a lot of theoretical and experimental efforts. In the past years, several mechanisms explaining fundamentals of HE have been reported [1]. According to them, possible explanations essentially rely on an interplay between hydrogen and lattice defects of different complexity (vacancies, surfaces, grain boundaries, dislocations) occurring in the material [2]. To complement existing viewpoints on the HE one needs to clarify possible changes in hydrogen diffusion near an isolated defect. Moreover, hierarchy of H diffusion coefficients related to different trap sites might be used for parametrization of the structure-specific models exploring hydrogen permeation in iron and steel [3,4]. Here we apply classical atomistic simulations to compare hydrogen diffusion in two different iron phases (bcc α-Fe and fcc γ-Fe) in presence of two-dimensional defects: tilt grain boundaries (GBs) and open surfaces. We also widen the topic by presenting the equilibrium hydrogen concentrations directly estimated for grain boundaries in bcc Fe. With that we detail a role of GB in the overall diffusion of hydrogen in this phase. Furthermore, we report diffusion coefficients illustrating changes in vacancy diffusion due to presence of hydrogen and discuss details of vacancy-hydrogen interaction in α and γ phases leading to such change.

2. Methodology and results

All results reported in this work were obtained from classical molecular dynamics (MD) simulations at finite temperatures. Calculations were carried out with LAMMPS Molecular Dynamics Simulator [5]. Interatomic interactions in Fe-H system were described with the recently reported classical angular-dependent potential for the ternary Fe-Cr-H system [6]. From the extensive simulations of Fe properties performed with this potential previously in [7] one may see that the model ensures proper stability regions for γ-Fe and α-Fe. Hence, it creates a unique opportunity for direct comparison of diffusion-related phenomena in these phases within the same methodological framework. In the following sections, we consider three different cases illustrating impact of hydrogen-defect interaction on H diffusion in Fe at finite temperatures. For each of the cases simulations were carried out for fcc and bcc Fe in parallel. Here we concentrate mainly on the aspects of diffusion since a question of hydrogen segregation on the considered defects has been already discussed (with estimation of the corresponding segregation energies) in our previous work [6].

* Corresponding author.
E-mail address: d.smirnova@mpie.de (D. Smirnova).
[1] Currently in Max-Planck-Institut für Eisenforschung GmbH, Max-Planck-Str. 1, 40237, Düsseldorf, Germany

https://doi.org/10.1016/j.commatsci.2023.112433
Received 10 March 2023; Received in revised form 7 August 2023; Accepted 8 August 2023
Available online 24 August 2023
0927-0256/© 2023 Elsevier B.V. All rights reserved.

2.1. Hydrogen diffusion in grain boundaries

Simulations performed by means of DFT [8] and classical methods [9,10] have shown that due to high segregation energy GBs can work as effective trapping sites for hydrogen. Same conclusion has been obtained from the experimental thermal analysis of hydrogen trapped in polycrystalline α phase [11]. Hence, one might expect that presence of GBs has influence on the overall diffusion of hydrogen in a system. Experimentally, such question has been addressed in [12]. In that work time-dependent distribution of hydrogen in a polycrystalline sample of pure α-Fe has been observed in situ by the silver decoration technique indicating the process of hydrogen permeation. The authors detected a high concentration of hydrogen in GBs, compared to that in bulk, which was suggested to be related to higher mobility of hydrogen along the GBs. However, owing to affinity of H to GBs, observed hydrogen distribution can be also explained at the expense of distinct H trapping, unassisted with accelerated H mobility along the defect. Also, according to the discussion given in [13–15], the experimental results might be interpreted through other phenomena possibly occurring in the vicinity of GBs in the sample. This includes introduction of micro-cracks due to formation of hydrogen atmospheres, accumulation of the plastic deformation in the process of charging, or creation of the dislocations assisting H migration. To assess the difference between H diffusion in GB and in bulk Fe, we performed a series of classic MD simulations of the isolated GBs populated with hydrogen. Namely, we considered symmetric tilt GBs with following orientations: (210)[001], (310)[001] and (510)[001]. To construct atomistic models of the GBs, two parts of a single crystal (i.e. grains) were rotated around the chosen tilt axis, and connecting plane represented a grain boundary. The equilibrium structures of GBs were prepared with γ surface method [16] followed up by annealing at finite temperature. Each simulation cell has been constructed with periodic boundary conditions (PBC) applied in all three directions, so a cell contained two identical GBs of the given orientation. For each given temperature, size of the simulation cell ensured zero-pressure conditions. Simulation cells contained about 30,000 atoms. The exact number was between 28,800 and 38,400 atoms depending on the host lattice structure (fcc or bcc) and chosen GB orientation. For the diffusion simulations, single hydrogen atom was placed in a random bulk position near each of the GBs (i.e. two H atoms diffuses in each calculation cell ensuring improved statistics). To estimate diffusion coefficients D_H, displacement of H atoms in a simulation box has been traced and averaged during the finite-temperature simulations in NVE ensemble. Diffusion coefficient for H in the GB was estimated using Eq. (1):

$$D_H = \langle R_H^2 \rangle / 2dt, \tag{1}$$

here $\langle R_H^2 \rangle$ is a mean squared displacement (MSD) of the hydrogen atoms in the simulation box during the time t; d — parameter related to the system dimensions: $d = 2$ for two-dimensional diffusion in the grain boundary or at surface, and $d = 3$ for bulk. Hydrogen migration was simulated for a total time of 10 ns. During the calculation MD trajectory was split into 10 equal parts (corresponding to $t = 1$ ns) by resetting the MSD and the calculation time to zero. Such approach gave us 10 independent trajectories describing H migration. The MSD averaged over the 10 trajectories was used to obtain D_H in the GB plane. It should be noted that in the simulation we observe two-dimensional nature of H migration in the GB plane. Displacement in the direction normal to the GB plane is negligible, as it is illustrated by sequence of H positions plotted in Fig. 1.

In Figs. 2(a) and 2(b) we plotted coefficients D_H estimated for GBs in bcc α-Fe and fcc γ-Fe. For bcc GBs, the simulations show noticeable drop in D_H compared to bcc bulk (this effect is especially evident at low temperatures). It means that in a wide temperature range grain boundaries in α-Fe do not provide fast diffusion channels for hydrogen migration, at the same time acting as strong traps for H. This result is consistent with the conclusion obtained previously

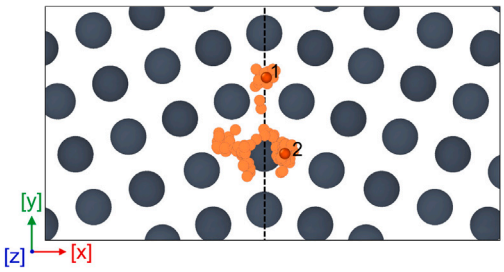

Fig. 1. Illustration of H interstitial diffusion in GB(210)[001] for bcc Fe at 400 K: large circles show positions of Fe atoms; 1 — position of H atom at $t_1 = 0$; 2 — position of H atom at $t_2 = 1.25$ ps. Small orange circles indicate the intermediate positions of H atom between t_1 and t_2.

from the classic simulations of different GBs in α phase [13]. For fcc γ-Fe our results are strictly opposite: mobility of H atom along GBs is higher than that inside a bulk. This trend can be clearly traced even when available temperature range is narrow because of a limited γ-Fe phase stability. Some scattering in the obtained data seen in Fig. 2 can be explained by the stochastic nature of MD simulations. Joint consideration of hydrogen diffusion in two different iron phases, as it is shown in Fig. 2, leads to a following general conclusion: according to the simulations, hydrogen migration enhances in fcc GBs and slows down in bcc GBs. At that, the values of D_H in fcc and in bcc bulk may set the temperature-dependent limits for possible variation in D_H due to the presence of tilt GBs. Since this result is obtained for isolated defects, it can be used for implementing the difference between bulk and GB diffusion, as introduced in hydrogen permeation models with explicit parametrization.

Fig. 2 shows difference between average H diffusion coefficients in different GBs. By calculating D_H plotted in Fig. 2 we used total displacements of H in the plane. This approach does not reflect details of the anisotropy expected for a diffusion in GB plane [17]. Additional analysis of the anisotropy degree for H diffusion was carried out by studying the diffusion of H parallel ($D_H^{\parallel}$) and perpendicular ($D_H^{\perp}$) to the GB tilt direction. As Fig. 3 shows, the degree of anisotropy $D_H^{\parallel}/D_H^{\perp}$ depends on GB structure and may change with temperature. Variations in the ratio observed in the simulations show that dominating direction of diffusion may be also a subject of change. For GBs in bcc, H migrates mainly along the tilt direction rather than in perpendicular direction. For GB(210) and GB(310), the difference between $D_H^{\parallel}$ and $D_H^{\perp}$ is of the order of 10. The most prominent anisotropy is seen for GB(510), where $D_H^{\parallel}/D_H^{\perp}$ is about 100 at $T \approx 450$ K and is completely anisotropic at lower temperatures. For GBs in fcc Fe, $D_H^{\parallel}$ was higher than $D_H^{\perp}$ only for GB(510), but the ratio $D_H^{\parallel}/D_H^{\perp} \leq 1$ was obtained for two other GBs.

2.2. Hydrogen diffusion on surfaces

Another case related to a question of hydrogen-invoked fracture and decohesion is hydrogen diffusion at surface. Surfaces are also reported to be strong trapping sites for H [18], and characterization of surface-related processes is required for describing fracture-related phenomena. Here we applied MD to observe character of hydrogen diffusion at Fe surfaces with different orientation. For this purpose, we built a series of simulation cells representing bcc and fcc Fe with free surfaces orientated normal to (100) and (110) lattice directions. The models of bcc (100) and (110) surfaces contained 3900 atoms and 7850 atoms, respectively, with PBC applied in two directions parallel to the surfaces. Similarly to the case of GBs, diffusion of H atom on the surfaces has two-dimensional character and exhibits no pronounced permeation in bulk. From the values of $\langle R_H^2 \rangle$ related to the H migration observed in the models, we produced D_H shown in Fig. 4. For bcc Fe D_H noticeably depends on the surface orientation accelerating for

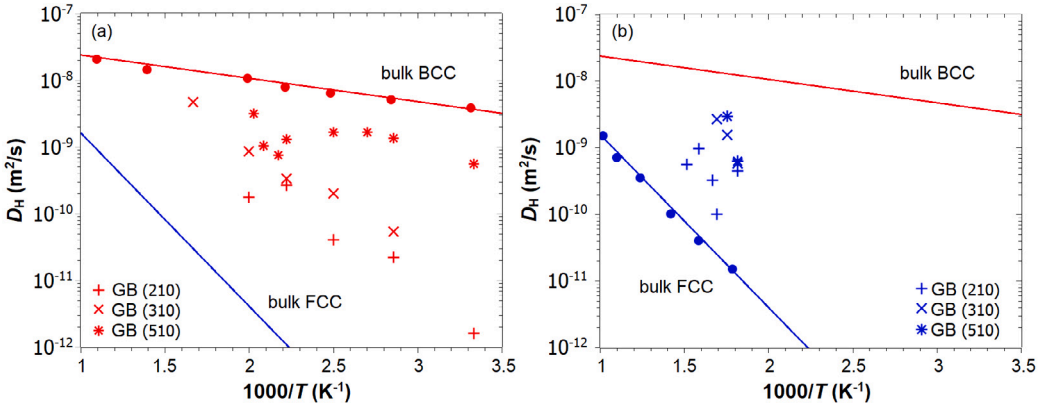

Fig. 2. Hydrogen diffusion coefficients D_H at different tilt grain boundaries: (a) — calculations for bcc Fe, (b) — calculations for fcc Fe. Solid lines corresponding to the temperature-dependent D_H calculated in bulk phases (denoted as •) are to guide the eye. Results for bcc are shown in red, for fcc — in blue.

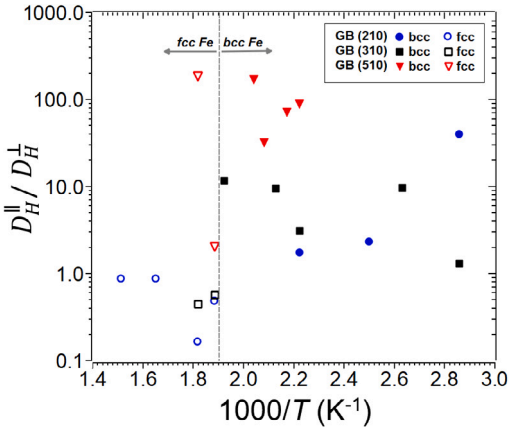

Fig. 3. Ratio between H diffusion coefficients estimated in the symmetric tilt grain boundaries. $D_H^{\parallel}$ — diffusion parallel to tilt direction, $D_H^{\perp}$ — diffusion perpendicular to tilt direction. Types of the GBs are encoded by symbols shown in legend. In the considered cases hydrogen does not migrate out of the GB plane.

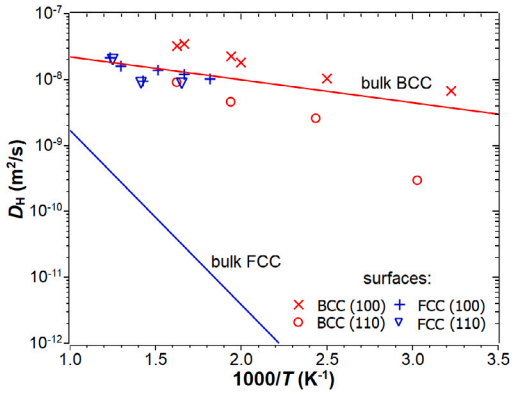

Fig. 4. Hydrogen diffusion coefficients D_H at (100) and (110) surfaces compared with diffusion in bulk Fe. Results for bcc and fcc structures are defined in red and blue, respectively.

(100) and decreasing for (110), nevertheless remaining in the vicinity of the values calculated for the bulk. The only exception is for (110) surface at room temperature where H migration is significantly suppressed. A small acceleration in H diffusion observed at the (100) surface compared to bulk is consistent with the MD calculations made specifically for this surface orientation by Liu et al. in [19] by means of different interatomic model [18]. At the same time, D_H estimated for the fcc crystal surfaces shows no pronounced dependence on the surface type and is in general several orders of magnitude higher than D_H in fcc bulk. Such effect might be interpreted as a way for hydrogen diffusion enhancement at the surfaces of fcc Fe. As well as the case of GBs, simulation of surfaces not only demonstrates a possibility of significant changes in H diffusion due to presence of these defects, but also sheds light on a noticeable difference in such phenomena depending on the structure of Fe phase. Furthermore, we can link the simulation results to the interpretation of aforementioned permeation experiments [12]. Namely, considering a hypothesis of cracks-assisted acceleration in H migration near the GBs: according to our simulations, presence of surfaces in bcc Fe would not increase a rate of H migration, so crack surfaces would provide a trap but probably not a source for enhanced H diffusion.

2.3. Cooperative diffusion of a single vacancy and H interstitials

According to the experiments and simulations [18,20], a mono-vacancy in α-Fe is capable of attracting up to six hydrogen atoms simultaneously [21]. Related hydrogen segregation energies for a case of mono-vacancy in this phase have been reported previously in the paper on the interatomic potential [6]. For a vacancy-H binding in γ-Fe, in this work we obtained corresponding energy $E \approx 0.4$ eV. An impact of pronounced bonding on diffusion of vacancy in bcc Fe has been considered previously in the study [22], which employed classical atomistic simulation and tight binding. In the other recent study [23] based on the off-lattice kinetic Monte Carlo model the same phenomena in α-Fe has been considered from different point of view. The kMC model was used for tracing the aspects of vacancy clusters diffusion in presence of a single hydrogen atom. Both works [22,23] mentioned possibility of a slow-down for a vacancy-H cluster in bcc lattice compared to diffusion of a mono-vacancy. Here, we continue investigation of related phenomena without restriction to only bcc Fe. We also include γ-Fe into consideration. The study covers up to three representative cases for a mono-vacancy diffusion: in pure Fe, at presence of 1 H atom, and at presence of 2 H atoms. The simulated system contained 1023 atoms for bcc Fe and 499 atoms for fcc Fe (with PBC applied in all directions). The systems were equilibrated at finite temperatures and zero pressure, then vacancy diffusion simulations were carried out in NVE ensemble. The efficient vacancy diffusion coefficient (D_{vac}) was extracted from the sum of squared displacements (δr_i^2) of all N Fe atoms in the simulated system. Calculation time t equals to 100 ns for α-Fe and 450 ns for γ-Fe:

$$D_{vac} = \sum_{i=1}^{N} \delta r_i^2 / 6t. \quad (2)$$

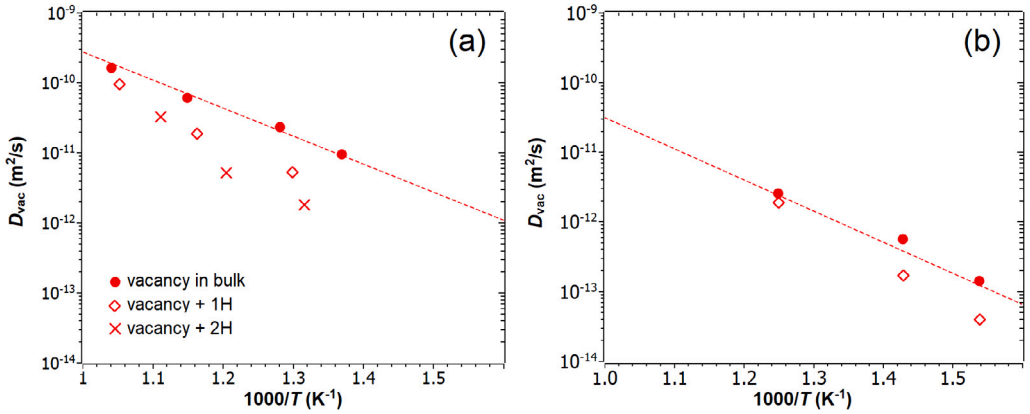

Fig. 5. Changes in vacancy diffusivity depending on number of H atoms in a system: panel (a) — calculations for bcc Fe, panel (b) — calculations for fcc Fe. Explanation of the symbols are given in the panels. Dashed lines are to guide the eye.

According to Fig. 5, presence of H atoms suppresses diffusion of a mono-vacancy in Fe. Such effect is seen regardless of the phase structure, however underlying diffusion mechanisms appears to be phase-specific. For α-Fe, the vacancy diffusion in presence of H takes place as the migration of a strongly bonded cluster. At the same time, binding of vacancy and hydrogen, as seen in simulations for fcc crystal, is noticeably weaker. Thus a vacancy and H atoms in γ-Fe migrate mostly as single defects experiencing occasional trapping slowing down the diffusion.

2.4. Hydrogen concentration at defects

Experimental observations of hydrogen permeation in polycrystal involve coupled processes of diffusion and segregation. A question about diffusion flux of hydrogen in defect-containing systems requires analysis of hydrogen concentration on crystal defects. Here, we considered a case of hydrogen concentration due to segregation at GBs in Fe. Namely, we calculated temperature dependence of hydrogen concentration (C_H^{GB}) at GB(210) and GB(310) in α-Fe. Here we discuss large-scale molecular dynamics simulations, which provide a general way to calculate the equilibrium hydrogen concentration in the presence of a crystal defect. These simulations were performed as a numerical experiment: model of a crystal containing grain boundary was slowly heated from 500 K to 1000 K. Total number of Fe atoms was about 360,000. Periodic boundary conditions were applied only in directions along the GB plane. To prevent hydrogen segregation on a free surface, several pre-surface atomic layers were fixed. For each GB type, we carried out simulations with two different bulk hydrogen concentrations: C_H^0 set to 0.001 and 0.005. Snapshots in Fig. 6a show computational cell used for simulation of GB(210) at $C_H^0 = 0.005$.

A main calculation stage was preceded by preliminary annealing stage. Annealing was necessary to achieve the equilibrium concentration of H inside the GB for the initial state. The annealing stage at $T = 500$ K took 30 ns, that was sufficient to achieve saturation of H atoms segregated at the GB. At the same time, the bulk concentration of H changed only by about 15 percent maximum (in the most extreme case for GB(210) and $C_H^0 = 0.001$). During the main calculation stage the model was heated with a constant rate of 12 K/ns. Here C_H^{GB} was calculated as ratio ρ_H/ρ_{Fe}, where ρ_{Fe} is bulk atomic density of Fe atoms and ρ_H is hydrogen atomic density in the orthogonal region around the GB. Thickness of the region in the direction perpendicular to the GB plane equals $h = 1$ nm. Fig. 6b shows calculated temperature-dependent ratio between the concentrations: C_H^{GB}/C_H^0. It is important to note that simulations with different C_H^0 led to the same temperature dependency. The calculated data can be described by the following equation: $C_H^{GB}/C_H^0 = \exp(S_{eff}/k_B) \cdot \exp(E_{eff}/k_BT)$ with the effective entropy S_{eff} and the effective segregation energy E_{eff} (k_B is Boltzmann constant). Based on the simulation results, the entropy and the energy are equal to $0.1k_B$ and 0.22 eV for GB(210), and $0.5k_B$ and 0.13 eV for GB(310). In fact, this numerical experiment allows us to determine the equilibrium concentration of hydrogen at GB for a given temperature and C_H^0. We also see that the obtained effective energies are lower than the segregation energy estimated for the most profitable sites in the considered GBs: 0.33 eV for GB(210) and 0.42 eV for GB(310) [6]. Such difference might be related to complex landscape of the trap sites filled at high temperature. The obtained concentration dependency can be easily transferred into the planar H concentration at GB (in atoms/nm^2):

$$C_H^{GB-pl} = h \cdot C_H^0 \cdot \rho_{Fe} \cdot \exp(S_{eff}/k_B) \cdot \exp(E_{eff}/k_BT)$$

Hydrogen flux J_H along diffusion channel is proportional to the combination $C_H \cdot D_H$. Based on the obtained results, we were able to compare bulk hydrogen flux J_H^0 with a flux J_H^{GB} along GB. Namely, for the two GBs, we can estimate $J_H^{GB}/J_H^0 = C_H^{GB} D_H^{GB}/C_H^0 D_H^0 \approx 1$ at all considered temperatures, so these fluxes are comparable. Since the total area of the GB channel is usually much smaller than the area of the bulk channel, the contribution of GBs to the total hydrogen flux for α-Fe can be considered negligible.

3. Discussion

With the help of classical finite-temperature atomistic simulations we studied hydrogen diffusion in α-Fe and γ-Fe in presence of isolated defects of several types: symmetric tilt GBs, surfaces, and a single vacancy. In case of GBs, hydrogen behavior not only depend on the GB orientation, but shows alternating trend depending on the bulk lattice type. For bcc Fe, introduction of the GBs does not provide fast channels for interstitial hydrogen diffusion, while for fcc Fe the situation is completely opposite. Moreover, surfaces in fcc Fe also may play an important role in accelerating H diffusion, while for bcc Fe such effect is not so evident. Results of the atomistic simulations confirm that interaction of hydrogen with defects does not follow some general low, but is strongly structure-specific. Among the cases considered in this work, only vacancy-H interaction keeps the same character for two studied Fe phases. Namely, due to pronounced vacancy-H bonding presence of H atom leads to reduction in vacancy diffusion coefficient. Calculated diffusion coefficients confirm previously reported results for bcc Fe and extend the same effect to the fcc structure. In this manner, isolated consideration of different defect types (together with bulk) allows to set up a consistent hierarchy of H diffusion coefficients, which might be used in further experimental and theoretical study of H permeation.

In terms of the permeation models, diffusion coefficients for α and γ phases reported in current work can be implicitly considered as numerical parameters contributing to the link between atomistic simulations

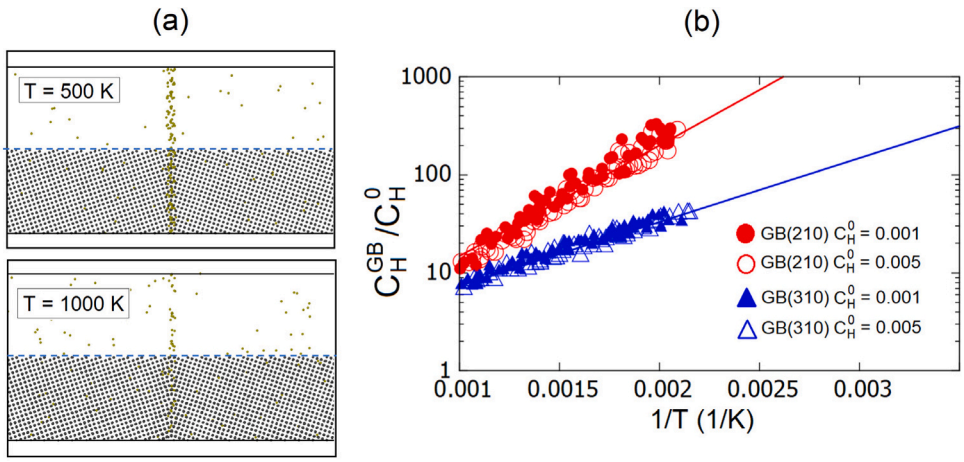

Fig. 6. (a) Computational cell containing GB(210) in bcc Fe: the snapshots show atomic positions at different temperatures. In each of the pictures, lower part shows all atoms, whereas in the upper part only H atoms (in orange) are shown. (b) Concentration ratio C_H^{GB}/C_H^0 calculated for different GB configurations at two different C_H^0. Solid lines determine analytical solution discussed in the text.

and higher-scale models of hydrogen permeation in polycrystalline iron. Moreover, reported data on H concentration and diffusivity at the defects may contribute to interpretation of the existing experiments [12,24] on H permeation in bcc Fe. Namely, for bcc Fe we show that GBs of the considered type do not act as diffusion accelerating channels. Such result agrees with the other atomistic calculations for the same phase referred to in the course of the paper. Based on this we may assume that the picture of H permeation observed in situ in [12], is probably a result coming from combination of fast H diffusion in bulk and strong segregation occurring at GBs. Our explanation differs from the original one [12], where the measurement data were interpreted as the result of quantitative similarity between bulk and GB diffusion coefficients.

The relationship between total hydrogen flux in GB and in interior of the grain has been also a matter of question in the experimental works [12,24]. To consider the picture in full we compared related hydrogen fluxes taking into account H concentration estimated in the given GB and in bulk. We show that the fluxes for GB and bulk are comparable, however, a role in the overall H flux is determined by the area of the related diffusion channels. Since the area of GBs is of a smaller order, overall diffusion in polycrystal will be governed by the term related to the grain interior. For bcc Fe this makes no significant difference from a single crystal. Thus, based on simulations results, we can conclude that almost identical H diffusion coefficients observed for single- and polycrystals in [24] can be explained by the insignificant contribution of the GB flux to the total H flux due to the small fraction of the GB area in the total diffusion area.

Declaration of competing interest

We wish to confirm that there are no known conflicts of interest associated with this publication and there has been no significant financial support for this work that could have influenced its outcome.

Data availability

Data will be made available on request.

Acknowledgments

D.S. gratefully acknowledges the financial support under the scope of the COMET program within the K2 Center “Computational Material, Process and Product Engineering (IC-MPPE)” (Project No 859480). This program is supported by the Austrian Federal Ministries for Transport, Innovation and Technology (BMVIT) and for Digital and Economic Affairs (BMDW), represented by the Austrian research funding association (FFG), and the federal states of Styria, Upper Austria and Tyrol. The calculations were carried out on the computer cluster Vulcan (ICAMS Computing cluster).

References

[1] M.B. Djukic, G.M. Bakic, V.S. Zeravcic, A. Sedmak, B. Rajicic, The synergistic action and interplay of hydrogen embrittlement mechanisms in steels and iron: Localized plasticity and decohesion, Eng. Fract. Mech. 216 (2019) 106528.

[2] H.K.D.H. Bhadeshia, Prevention of hydrogen embrittlement in steels, ISIJ Int. 56 (2016) 24–36.

[3] A. Drexler, W. Siegl, W. Ecker, M. Tkadletz, G. Klösch, H. Schnideritsch, G. Mori, J. Svoboda, F.D. Fischer, Cycled hydrogen permeation through armco iron–a joint experimental and modeling approach, Corros. Sci. 176 (2020) 109017.

[4] A. Díaz, I. Cuesta, E. Martinez-Pañeda, J. Alegre, Analysis of hydrogen permeation tests considering two different modelling approaches for grain boundary trapping in iron, Int. J. Fract. 223 (2020) 17–35.

[5] A.P. Thompson, H.M. Aktulga, R. Berger, D.S. Bolintineanu, W.M. Brown, P.S. Crozier, P.J. in’t Veld, A. Kohlmeyer, S.G. Moore, T.D. Nguyen, et al., LAMMPS - a flexible simulation tool for particle-based materials modeling at the atomic, meso, and continuum scales, Comput. Phys. Comm. 271 (2022) 108171.

[6] S. Starikov, D. Smirnova, T. Pradhan, I. Gordeev, R. Drautz, M. Mrovec, Angular-dependent interatomic potential for large-scale atomistic simulation of the Fe-Cr-H ternary system, Phys. Rev. Mater. 6 (2022) 043604.

[7] S. Starikov, D. Smirnova, T. Pradhan, Y. Lysogorskiy, H. Chapman, M. Mrovec, R. Drautz, Angular-dependent interatomic potential for large-scale atomistic simulation of iron: Development and comprehensive comparison with existing interatomic models, Phys. Rev. Mater. 5 (2021) 063607.

[8] A.S. Kholtobina, W. Ecker, R. Pippan, V.I. Razumovskiy, Effect of alloying elements on hydrogen enhanced decohesion in bcc iron, Comput. Mater. Sci. 188 (2021) 110215.

[9] X.-Y. Zhou, X.-S. Yang, J.-H. Zhu, F. Xing, Atomistic simulation study of the grain-size effect on hydrogen embrittlement of nanograined Fe, Int. J. Hydrogen Energy 45 (2020) 3294–3306.

[10] M. Rajagopalan, M. Tschopp, K. Solanki, Grain boundary segregation of interstitial and substitutional impurity atoms in alpha-iron, Jom 66 (2014) 129–138.

[11] W. Choo, J.Y. Lee, Thermal analysis of trapped hydrogen in pure iron, Metall. Trans. A 13 (1982) 135–140.

[12] M. Koyama, D. Yamasaki, T. Nagashima, C.C. Tasan, K. Tsuzaki, In situ observations of silver-decoration evolution under hydrogen permeation: Effects of grain boundary misorientation on hydrogen flux in pure iron, Scr. Mater. 129 (2017) 48–51.

[13] S. Teus, V. Gavriljuk, Grain-boundary diffusion of hydrogen atoms in the α-iron, Metallofiz. Noveish. Tekhnol. 36 (2014) 1399–1410.

[14] V. Gavriljuk, S. Teus, Comments to the paper in situ observations of silver-decoration evolution under hydrogen permeation: Effects of grain boundary misorientation on hydrogen flux in pure iron, the authors: M. Koyama et al. scripta mater 129 (2017) 48-51, Scr. Mater. 140 (2017) 88–90.

[15] M. Koyama, D. Yamasaki, K. Tsuzaki, Reply to comments on the paper in situ observations of silver-decoration evolution under hydrogen permeation: Effects of grain boundary misorientation on hydrogen flux in pure iron by gavriljuk and teus, Scr. Mater. 140 (2017) 91–92.
[16] V. Vitek, Intrinsic stacking faults in body-centred cubic crystals, Phil. Mag. 18 (1968) 773–786.
[17] Y. Mishin, Chr. Herzig, Grain boundary diffusion: recent progress and future research, Mater. Sci. Eng. A 260 (1999) 55–71.
[18] A. Ramasubramaniam, M. Itakura, E.A. Carter, Interatomic potentials for hydrogen in α–iron based on density functional theory, Phys. Rev. B 79 (2009) 174101.
[19] X. Liu, W. Xie, W. Chen, H. Zhang, Effects of grain boundary and boundary inclination on hydrogen diffusion in α-iron, J. Mater. Res. 26 (2011) 2735–2743.
[20] D. Jiang, E.A. Carter, Diffusion of interstitial hydrogen into and through bcc fe from first principles, Phys. Rev. B 70 (2004) 064102.
[21] A. Pundt, R. Kirchheim, Hydrogen in metals: Microstructural aspects, Annu. Rev. Mater. Res. 36 (2006) 555–608.
[22] S.E. Restrepo, H. Lambert, A.T. Paxton, Effect of hydrogen on vacancy diffusion, Phys. Rev. Mater. 4 (2020) 113601.
[23] C. Williams, E. Galindo-Nava, Accelerating off-lattice kinetic monte carlo simulations to predict hydrogen vacancy-cluster interactions in α-Fe, Acta Mater. 242 (2023) 118452.
[24] H. Hagi, Y. Hayashi, N. Ohtani, Diffusion coefficient of hydrogen in pure iron between 230 and 300 K, Trans. Japan Inst. Metals 20 (1979) 349–357.